J Mater Sci (2014) 49:70–78
DOI 10.1007/s10853-013-7662-5

Polyolefin-based nanocomposites: the effect of organosilane on organoclay dispersion

K. S. Santos · S. A. Liberman · M. A. S. Oviedo · R. S. Mauler

Received: 26 April 2013 / Accepted: 7 August 2013 / Published online: 17 September 2013

Abstract This work dealt with the morphology and properties of polypropylene/organoclay (PP/OMMt) nanocomposites prepared using maleic anhydride-grafted polypropylene (PP-*g*-MA) or organosilane (OTMS) as a compatibilizing agent. The content of OMMt was 2 wt%, and different concentrations of OTMS were used to obtain OTMS/OMMt mass ratios of 0/1, 1/1, 0.5/1 or 0.25/1. The results of wide-angle X-ray scattering and transmission electron microscopy investigations showed that the OTMS promoted the total exfoliation of OMMt in the PP matrix, while the OMMt yielded a micrometer-scale dispersion when PP-*g*-MA was used. In general, the OTMS satisfactorily compatibilized the PP/OMMt nanocomposites, increasing the modulus of the PP matrix. When a hybrid compatibilizer of OTMS/PP-*g*-MA was used, better thermal and mechanical properties were achieved.

Introduction

Polypropylene (PP) is one of the most widely used plastics in large-volume applications, but it presents some disadvantages, such as low toughness and low service temperatures [1]. One of the most interesting opportunities to improve the properties of isotactic polypropylene is combination with mineral and polymer material on a very fine structural level [2–4]. The incorporation of small amounts of inorganic fillers, such as montmorillonite modified with quaternary ammonium salt with long alkyl groups (OMMt), which possesses a multilayer structure and high aspect ratio, improves the final properties, increasing the mechanical resistance, thermal stability, and optical properties in addition to afford the material with better flame and barrier properties [1–6]. However, the degree of reinforcement depends largely on the interaction forces (the interfacial energy) between the polymer matrix and the clay [7].

OMMt is sufficiently delaminated by the action of shear tension, and therefore, melt intercalation in twin-screw extruders is the main method used to obtain OMMt nanocomposites [8]. The efficiency of the dispersion/distribution process depends on the temperature, residence time, and screw shear profile [1, 8]. The use of intermediate residence times, low processing temperatures, and medium shear rates are the best conditions for obtaining exfoliated and small agglomerated clay structures [8]. Further, the success of exfoliation by melt blending is associated mainly with the presence of strong interactions between the clay and the polymer chain [9]. The most critical condition for the formation of intercalated and, in particular, exfoliated structures via melt intercalation are the presence of polar interactions between the components [10]. The complete delamination of clay platelets in the PP matrix is a challenge because the mixture of these components is not favored thermodynamically [1]. The choice of the molecular weight of isotactic PP, the chemical modification of clay by organic cations (organophilization), and the best melting process conditions contribute to make the kinetics of intercalation between the PP and OMMt more favorable [1, 11]. The use of compatibilizing agents containing polar groups is necessary to promote additional enthalpy in the

K. S. Santos · R. S. Mauler (✉)
Instituto de Química, Universidade Federal do Rio Grande do Sul, Av Bento Gonçalves 9500, Porto Alegre, RS 91501-970, Brazil
e-mail: raquel.mauler@ufrgs.br

S. A. Liberman · M. A. S. Oviedo
Braskem S/A, III Pólo Petroquímico, Via Oeste Lote 5, Passo Raso, Triunfo, Brazil

process intercalating the PP into the organoclay [12–15]. However, to obtain higher platelet delamination in the polymer matrix in these ternary systems, it is necessary to optimize the amount of polar groups in the compatibilizer, the molecular weight of the compatibilizer and the compatibilizer/organoclay ratio [16–20]. Then, to achieve better interfacial adhesion, it is important that the compatibilizer chains entangle deeply with the matrix molecules, in addition to have a strong interaction with the filler [21, 22]. These compounds are usually based on polyolefins modified with maleic anhydride, acrylic acid, silanes, itaconic acid, glycidyl methacrylate, and other organic molecules, such as amines and chlorosulfonic acid, and the use of random or block copolymers [1, 2, 9, 23]. The PP-*g*-MA is the most common compatibilizer used to obtain PP nanocomposites with OMMt; however, because of its low molecular weight, the final properties of these materials can be diminished [1, 9]. Some studies have shown that, to achieve higher clay dispersions in the PP matrix, large concentrations of compatibilizer are necessary [1, 24]. Sanchez-Valdes et al. [24] produced PP nanocomposites with a 29 % increase in the modulus and a 58 % increase in impact strength using a 3:1 ratio of PP-*g*-MA and OMMt. However, previous studies in our laboratory showed that the 1:1 ratio of OMMt and PP-*g*-MA presented the best balance of mechanical properties for the PP nanocomposites [9]. Another compatibilizer agent that also has been studied to improve the adhesion between PP and OMMt is organosilane, which can be grafted onto the PP matrix or into the clay surface [25–37]. In addition, the combination of two different compatibilizers, PP-*g*-MA and organosilane, has been used in the preparation of PP nanocomposites. Liaw et al. [38] used this mixture with different proportions of 3-(aminopropyl) triethoxy silane (APTS) and PP-*g*-MA to prepare PP/OMMt nanocomposites with partial exfoliation, giving a 57 % increase of Young's modulus. They proposed a three-step process: first, APTS was allowed to react with PP-*g*-MA to form the compound coupling compatibilizer; second, the PP-*g*-MA/APTS compound coupling compatibilizer was allowed to react with the organoclay to form a hybrid masterbatch; third, the masterbatch was then compounded with neat PP to form the nanocomposite. The described processes summarize the inherent difficulty that is present in obtaining PP/OMMt nanocomposites with highly distinct final properties.

A new alternative for compatibilization between PP and OMMt is the direct addition of organosilane during the melt processing step, without performing a prior matrix or nanoclay functionalization step, i.e., the process uses only one step. This methodology looked for just one step to obtain the polymer nanocomposites and to get the necessary compatibility among the components, without previous PP or clay functionalization with organosilanes or without use of masterbatches. In this work, a physical mixture of PP with Cloisite (C) 15A or 20A in the presence of a small amount (0.5, 1 or 2 wt%) of trimethoxy(octadecyl)silane (OTMS) was performed to improve the dispersion of OMMt in the PP matrix. Further, a hybrid compatibilizer of 1.5 wt% of PP-*g*-MA with 0.5 wt% of OTMS was used to verify the effect of both compatibilizer agents on the dispersion of the PP/OMMt nanocomposites.

Experimental

Materials

Polypropylene (MFR (230 °C/2.16 kg) 3.5 g/10 min) was obtained from Braskem S.A; Irganox® B215 (antioxidant), from Ciba; maleated polypropylene (PP-*g*-MA) with a reactive MA modifier content 0.5 wt% (MFR (230 °C/2.16 kg): 50 g/10 min), from Chemtura; and trimethoxy(octadecyl)silane (OTMS) with a density of 0.883 g/cm^3, from Aldrich. The organophilic montmorillonites used were Cloisite® 15A (modifier concentration: 125 meq/100 g) and 20A (modifier concentration: 95 meq/100 g), obtained from Rockwood Additives.

Melt processing

The mixtures were prepared using melt intercalation in a counter-rotating twin-screw extruder (Coperion ZSK18K38, screw diameter of 18, L/D = 44) operating at 350 rpm with a constant feed ratio of 3 kg/h and a temperature profile of 165, 170, 175, 175, 180, 185, 190°C with 2 wt% of OMMt (either C15A or C20A). The nanocomposites were molded in accordance with ASTM D-638 type 1 in a Battenfeld Plus 350/075 injection molding machine. The temperature of the cylinders ranged from 220 to 230 °C, and the mold was held at 60 °C. Films were obtained by compressing the polymer at a temperature up to 190 °C, maintaining compression for 2 min to obtain completely melted pellets, followed by the application of 6 lbs of pressure for 3 min. The sample was then cooled to room temperature at a cooling rate of approximately 20 °C/min.

Characterization

Wide-angle X-ray scattering (WAXS) experiments were performed on a Siemens D-500 diffractometer. Films (PP nanocomposites) and powder (organoclays) were scanned in reflection mode using an incident X-ray beam of CuK_α with a wavelength of 1.54 Å at a step width of 0.05°/min from $2\theta = 1$ to 10°. The basal spacings of the clays and PP

nanocomposites were estimated from the (001) reflections. The morphologies of the specimens were examined by TEM (JEOL JEM 120 Ex II) operated at an accelerating voltage of 80 kV. Ultra thin specimens (70 nm) were cut from the mid sections of the injection-molded specimens, perpendicular to the flow direction of melt during the injection process. The cutting operations were carried out with a RMC CXL microtome under cryogenic conditions; the system was equipped with a glass or diamond knife. The cutting operations were performed at −80 °C, and each film was retrieved onto a 300 mesh Cu grid. The TEM images, which were typically magnified 30,000 times, were quantified using Adobe Photoshop: the dispersed platelets and/or agglomerate structures captured through TEM were traced over onto an overlaying blank layer. To insure accurate measurements of the particle length and thickness dimensions, the images were sufficiently magnified so that a majority of the particles, including individual platelets, could be counted by the Image Tools program.

The thermal behavior of the specimens was determined using a DSC thermal analyst 2100/TA Instrument. All measurements were carried out in nitrogen atmosphere. The samples were heated from 50 to 200 °C at heating and cooling rates of 10 °C/min. The measurements were performed in the second heating and cooling cycle. The degree of crystallinity was determined using $\Delta H_m^0 = 190$ J/g for PP [39]. Thermogravimetric analyses were carried out on a TA model QA-50 to obtain the inorganic and organic residues in addition to the decomposition profiles of the clays and PP nanocomposites. The samples (10.0 ± 0.3 mg in film form) were heated from 80 to 900 °C at 20 °C/min under nitrogen flow.

A TA model QA 800 instrument was used for dynamic mechanical analyses (DMA), and the heat deflection temperature (HDT) behavior of the materials was fixed at the frequency of 1 Hz. DMA analyses were performed in the single cantilever mode. The injection-molded samples were heated from −30 to 130 °C at a heating rate of 3 °C/min. The HDT was estimated from the DMA results, according to the methodology proposed by Scoboo [40, 41]. The HDT is defined by ASTM standards (D648) as the temperature at which the center deflection of a standard specimen in a three-point bend mode reaches 0.25 mm under an applied maximum stress of either 0.46 or 1.82 MPa. The condition of 1.82 MPa stress was selected because it is typically employed for semi-crystalline and filled polymers. The HDT at the stress of 1.82 MPa corresponds to the temperature at which the logarithm of storage modulus is 8.9 or 794 MPa. Tensile testing was performed according to ASTM D638, specimen type 1, conducted on a universal tensile machine (EMIC DL 10000) at a crosshead rate of 50 mm/min using an extensometer. Izod Impact tests were performed at 23 °C using a pendulum-type impact tester (Ceast, Resilimpact) according to ASTM D 256. The reported values are averaged from 10 individual measurements.

Results and discussion

Nanocomposite morphologies

The nanocomposite morphology is affected by several factors, such as the preparation method, the processing conditions, the shear stress, the matrix molecular weight, the structure of the organic modifier, and the compatibilizers used [1]. Thus, the use of OTMS mixed with organoclay modifies the morphology and consequently the final properties of the PP nanocomposites.

Wide-angle X-ray scattering

The WAXS results of C15A and the nanocomposites prepared with 2 wt % OMMt, without or with PP-*g*-MA, and OTMS (mass compatibilizer/mass organoclay = 1) are shown in Fig. 1 and Table 1. The profiles for the organoclay and PP/C15A/PP-*g*-MA nanocomposite show wide single basal reflections due to the random orientation of the organoclay platelets, while the profile of the PP/C15A/OTMS sample shows narrower peaks and higher order reflections, indicating the higher level of organization and orientation of the clay structures.

The use of OTMS promoted an increase of 18 % in the interlayer distance (from 3.39 to 4.01 nm), indicating the higher interaction of this compatibilizer with the silicate, which was due to the chemical reaction that occurred between methoxysilane and the Si–OH groups that are

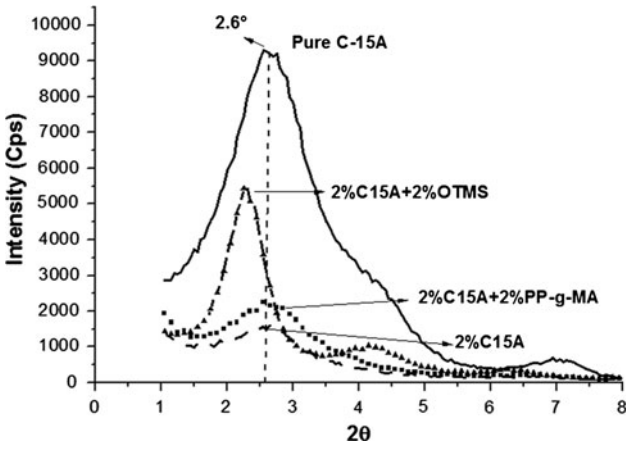

Fig. 1 XRD patterns of the 2 wt% C15A and PP nanocomposites: without a compatibilizer, with PP-*g*-MA and with OTMS

Table 1 The interplanar distances of 2 wt% C15A and its nanocomposites: without a compatibilizer, with PP-*g*-MA and with OTMS

Samples	2θ	d_{001} (nm)
C15A	2.6	3.39
2 % C15A	2.6	3.39
2 % C15A + 2 % PP-*g*-MA	2.6	3.39
2 % C15A + 2 % OTMS	2.2	4.01

exposed on the clay edge surfaces [33]. This effect is not observable with PP-*g*-MA because its high molecular weight does not favor intercalation into the OMMt galleries.

Transmission electron microscopy and particle analysis

A better understanding of the dispersion and orientation of the clay platelets in the PP matrix can be gleaned from TEM analysis [1, 42]. This technique enables an evaluation of the clay particle aspect ratio, which is one of the most important factors in determining the reinforcement efficiency of the clay [10, 43]. In particular, this value is a maximum when the parallel-exfoliated platelets are uniformly oriented [44]. In addition to the orientation evaluation, the number of agglomerates and the spacing between the OMMt platelets also can be obtained using TEM analysis [2]. Figure. 2 shows representative TEM micrographs for the PP/2 % C15A nanocomposites without and with a compatibilizer, noted to be either PP-*g*-MA (PP-*g*-MA/OMMt = 1:1 w/w) or OTMS (OTMS/OMMt = 0.25, 0.5 and 1:1 w/w). The morphology of the PP/2 % C15A sample exhibits typical agglomerated structures of OMMt and a heterogeneous distribution in the absence of a compatibilizing agent (Fig. 2a). When either PP-*g*-MA or OTMS was added, better dispersion of the clay was achieved, as can be observed in Fig. 2b–e). The degree of exfoliation and distribution of OMMt with OTMS was significantly higher than that obtained with PP-*g*-MA. The use of a larger amount of OTMS did not result in significant improvements in the dispersion of C15A in comparison to that achieved with 0.5 wt% of OTMS. The use of a hybrid compatibilizer (0.5% OTMS and 1.5 % PP-*g*-MA) promoted nearly complete exfoliation of C15A clay in the PP matrix (Fig. 2f). The clay particles were well aligned in the flow direction for all systems investigated.

Further, the degree of interaction between the compatibilizer polar groups and the clay surface is directly related to the amount of organic modifier present between the clay layers [1, 2, 8]. To evaluate the effect of the amount of organic modifier in the clay, C20A with the same type of ammonium salt but a lower surfactant amount than the C15A was used. The morphological aspects of the nanocomposite with this clay (C20A) and OTMS were similar to that of the PP/C15A nanocomposites (Fig. 3).

This behavior shows that the OTMS was able to interact with both organoclays, likely because it is capable of interacting with the hydroxyl groups on the clay surface in addition to the organic modifier. In the case of PP-*g*-MA, better performance was obtained with the less modified organoclay (C20A).

In addition, to evaluate the influence of the compatibilizer on the aspect ratio of the clay nanocomposites, statistical analyses of the TEM images were carried out, using a 30,000× magnification and a total area of 19.8 μm^2 (Fig. 2). The dispersion degree and the degree of clay distribution in the polymer matrix can be evaluated from the aspect ratio of the clay [2, 3]. As the amount of platelets with smaller lengths and thicknesses is increased, the dispersion grows better [2]. However, with higher delamination, the clay sheets can become bent over on themselves [3]. This creates difficulty in the dimensional analysis of these structures, but it is possible to establish some morphological trends. For increased validity of the statistical analysis, a significant number of particles must be analyzed for a given sample, i.e., ideally in the range of 400–500 particles [2]. Paul et al. [2] identified approximately 250 clay particles for PP/5 wt% OMMt nanocomposite systems using PP-*g*-MA. However, in less-exfoliated polyolefin nanocomposites containing low concentrations of clay (less than 5 wt%), this particle number is difficult to achieve [1, 3, 9]. In our case, approximately 20–150 particles could be counted to evaluate the length and thickness of the PP/2 wt% C15A nanocomposites. Figure 4a, b show typical histograms of the C15A particle distribution of terms of the lengths, thicknesses and statistical data obtained for the PP nanocomposites without a compatibilizer. Similar measurements were conducted for the other nanocomposites, but their histograms have been omitted. The standard deviation values of the measurements were high, indicating large distributions of the lengths and thicknesses in the PP nanocomposites. These results are consistent with the previous observations reported in the literature [2, 3, 33]. Based on the histograms of the nanocomposites, average values of the lengths and thicknesses of the OMMt particles in the PP matrix were established (Fig. 5).

The use of PP-*g*-MA produced better distribution and enhanced dispersion of OMMt in the PP matrix. These nanocomposites showed twice the number of particles of OMMt in comparison to the nanocomposites produced without PP-*g*-MA (i.e., an increase from 26 to 55 OMMt particles). The average length of the clay particles was not modified (350 nm), but the thickness was reduced by half (from 119 to 57 nm), which doubled the value of the aspect ratio. When OTMS was used, complete exfoliation was almost reached. The addition of 0.5 wt% of OTMS was

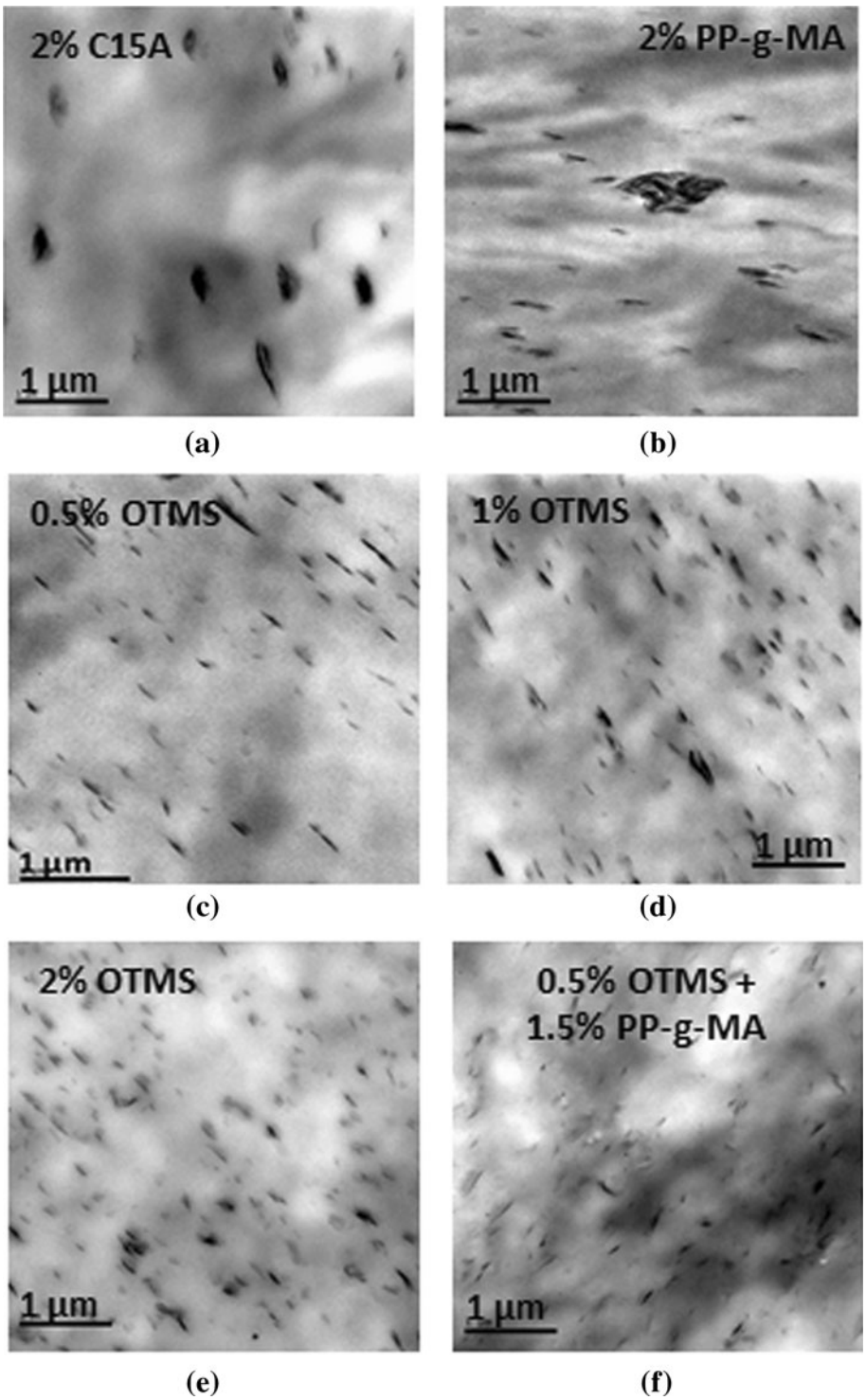

Fig. 2 TEM images (magnification: 30×) of the 2 wt% C15A/PP nanocomposites: without a compatibilizer (**a**), with 2 wt% PP-*g*-MA (**b**), with 0.5, 1, and 2 wt% OTMS (**c**–**e**) and the 1.5 wt% PP-g-MA/0.5 wt% OTMS hybrid (**f**)

sufficient to increase the number of particles of OMMt by a factor of four, reducing their thicknesses (from 119 to 19 nm) by a factor of six, and increasing the aspect ratio of the PP nanocomposites by a factor of three. However, as the number of sheets in the structure of OMMt was reduced, the average length grew smaller (200 nm).

Relationship of the PP nanocomposite morphologies with the thermal, mechanical dynamical, and mechanical properties

The degree of dispersion of the clay particles in the polymer matrix is directly related to the ability of the

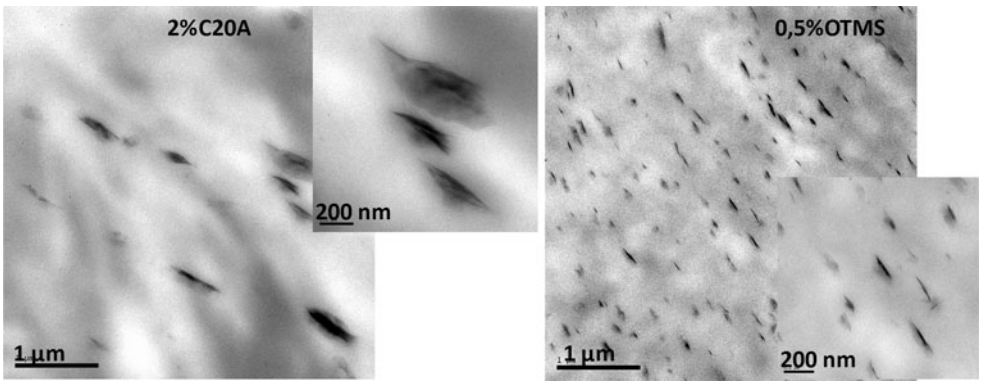

Fig. 3 TEM images (magnification: 30× and 100×) of the 2 wt% C20A/PP nanocomposites: without a compatibilizer (**a**) and with 0.5 wt% OTMS (**b**)

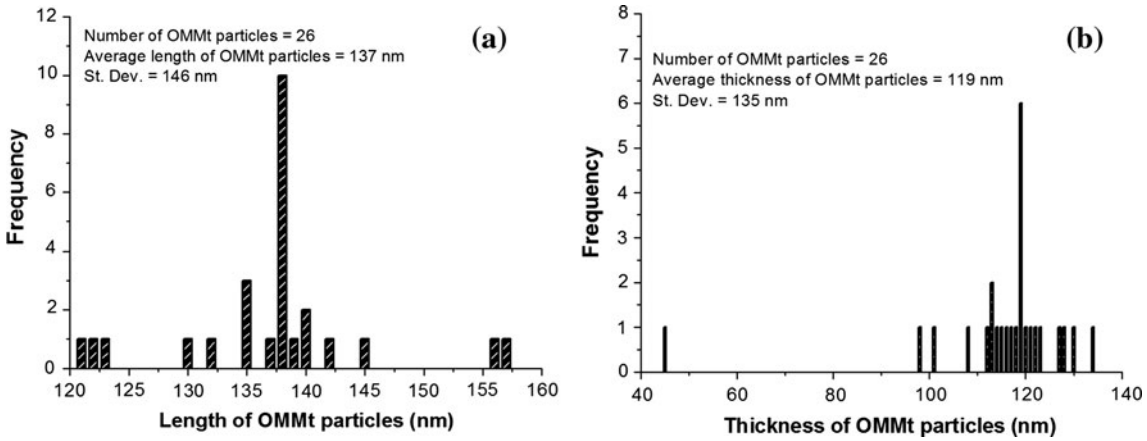

Fig. 4 A histogram of the number of OMMt particles (26 particles): length **a** and thickness, **b** in the PP/2 % C15A nanocomposites

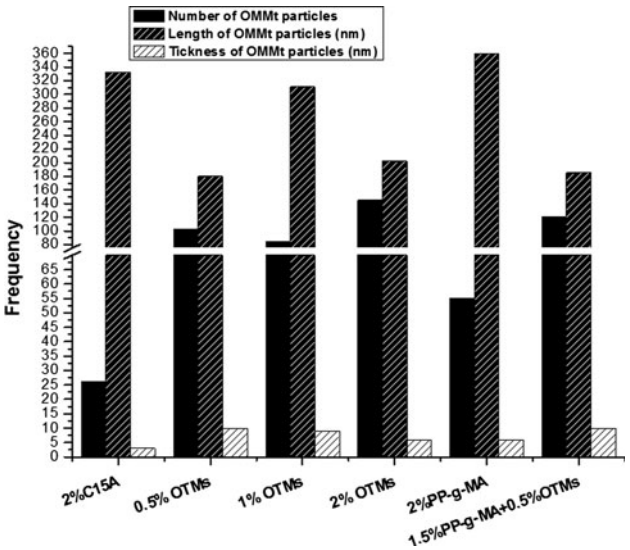

Fig. 5 A histogram of the average values of the lengths and thicknesses of the 2 wt% C15A particles in the PP nanocomposites: without a compatibilizer, with 2 wt% PP-*g*-MA, with 0.5, 1 and 2 wt% OTMS and the 1.5 wt% PP-*g*-MA/0.5 wt% OTMS hybrid

clay particles to delaminate, which in turn determines the aspect ratio (length/thickness) and the efficiency of reinforcement of the clay in the matrix [1]. The system with 2 wt% of OTMS, even with greater dispersion of the clay, only achieved a Young's modulus that was comparable to that of 2 wt% PP-*g*-MA (Table 2). This behavior is associated with the thinner OMMt structures that result from the use of OTMS, yielding greater flexibility and reducing the orientation of the clay sheets in the PP matrix. In addition, the OTMS has a low molecular weight, which fails to promote the effective entanglement of its chains with those of PP, consequently allowing the premature flow of PP chains during tensile test. This behavior was not suppressed by the use of the 0.5 and 1.5 % OTMS/PP-*g*-MA mixture. Intermediate nanocomposite aspect ratios presented enhanced reinforcement efficiency in the PP matrix (Fig. 6a). This result indicates that the reinforcement produced by the clay platelets in the polymeric matrix does not depend only on the aspect ratio (length/thickness) but is mainly

Table 2 The thermal, mechanical, and dynamical mechanical properties of neat PP and the PP nanocomposites

Samples	Young's modulus (MPa)	Storage modulus at 23 °C (MPa)	HDT at 794 MPa (°C)	Tc[a] (°C)	$T_{10\ \%}$ (°C)	$T_{50\ \%}$ (°C)	Izod impact at 23 °C (J/m)
Blank							
Neat PP	1697 ± 45	1118	41	113	380	436	45 ± 6
2 wt% C15A							
C15A	1835 ± 65	1324	50	115	420	460	55 ± 5
2 % PP-*g*-MA	2096 ± 85	1357	51	115	434	467	41 ± 4
0.5 % OTMS	1830 ± 53	1324	49	115	443	471	41 ± 7
1 % OTMS	1824 ± 24	1401	51	113	422	461	46 ± 5
2 % OTMS	1992 ± 46	1334	51	112	428	465	46 ± 6
1.5 % PP-*g*-MA + 0.5 % OTMS	1779 ± 46	–	–	115	–	–	58 ± 5
2 wt% C20A							
C20A	1831 ± 25	1358	50	115	396	456	51 ± 7
0.5 % OTMS	1926 ± 14	1390	51	114	462	476	56 ± 6

$T_{10\ \%}$ temperature at which 10 % of weight loss occurs, $T_{50\ \%}$ temperature at which 50 % of weight loss occurs

[a] Standard deviation ±1 °C

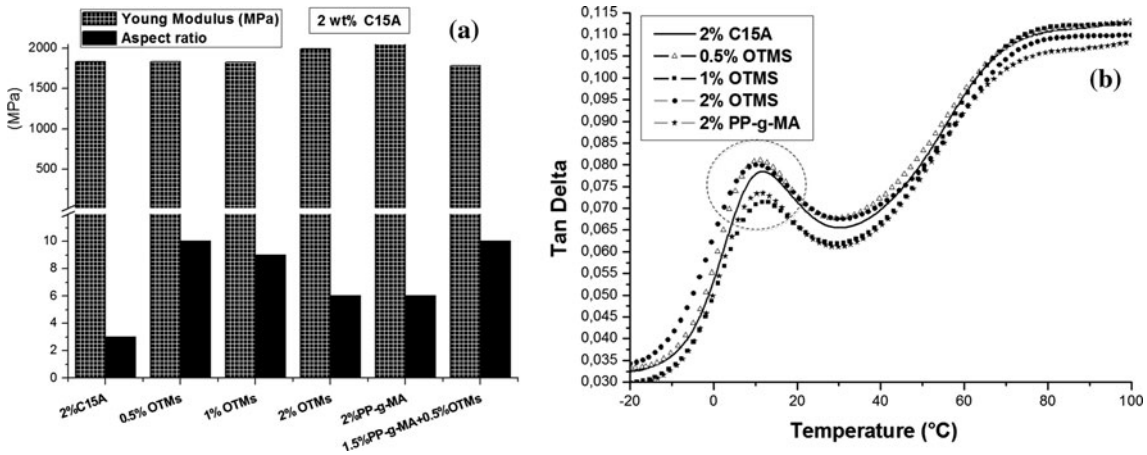

Fig. 6 The relationship between Young's modulus and aspect ratio **a** and tan δ, **b** of the 2 wt% C15A/PP nanocomposites: without a compatibilizer, with 2 wt% PP-*g*-MA, with 0.5, 1, and 2 wt% OTMS and the 1.5 wt% PP-*g*-MA/0.5 wt% OTMS hybrid

dependent on the force of adhesion between the components.

The results obtained using only 2 wt% OMMt and a single step showed an increase of 20 and 30 % in rigidity and in impact strength of PP, respectively. These increases are quite promising when compared with results already published elsewhere, using over 3 wt% OMMt, generally using two or more steps for the preparation of PP nanocomposites and showing the decrease in Izod impact [15, 25, 33, 38].

The PP nanocomposite storage modulus at 23 °C showed behavior similar to that of the Young's modulus (increased approximately by 20 % in comparison to neat PP). The β transition temperatures (T_g) of the nanocomposites (recorded at approximately 12 °C) were not changed by the clay addition or by the use of a compatibilizing agent (Fig. 6b). Further, the β transition peak intensity is related to relaxation of the amorphous segments of the PP chains, and it can indicate the interaction force that is present between the clay sheets and the PP chains [8]. The addition of 1 wt% OTMS or 2 wt% PP-*g*-MA promoted a decrease in the peak intensity of 2 % C15A, indicating stronger interactions between this clay-polymer system. However, the use of 0.5 or 2 wt% OTMS was insufficient to promote good adhesion between the filler-matrix system. The clay addition increased the HDT (approximately 10 °C), the T_c (which acted as a nucleation agent) and improved the impact strength, but it did not

change the melt temperature (T_m) or the crystallization degree (X_c) of the PP matrix (Table 2). The use of a compatibilizing agent did not alter the heat deflection temperature (HDT), the crystallization temperature (T_c) or the impact strength of the PP nanocomposites, except when the PP-*g*-MA/OTMS hybrid was used. However, the initial ($T_{10\ \%}$) and final ($T_{50\ \%}$) degradation temperatures were slightly improved using the compatibilizing agents. The C20A nanocomposites presented thermal, mechanical and dynamical mechanical behaviors that were slightly better than those of the PP/C15A nanocomposites.

Conclusion

PP nanocomposites were prepared using OMMt with different compatibilizing agents. The morphology of the PP nanocomposites exhibited agglomerated structures that are typical of OMMt platelets in addition to heterogeneous distributions in the absence of a compatibilizing agent. When either PP-*g*-MA or OTMS was added, better clay dispersion was achieved. The use of OTMS reduced the efficiency of OMMt dispersion in comparison to that of PP-*g*-MA, but its low molecular weight did not allow for sufficient entanglement of its chains with those of PP. The use of an increased amount of OTMS did not result in significant improvements in the dispersion of C15A in comparison with that obtained for 0.5 wt% of OTMS. The use of a hybrid compatibilizer (0.5 % OTMS and 1.5 % PP-*g*-MA) promoted complete exfoliation of the C15A platelets in the PP matrix. The OTMS was able to interact with any organoclay surface, because it interacts with both the hydroxyl groups on the clay surface and the organic modifier chains. The T_m and X_c were not affected by the presence of clay, PP-*g*-MA, or OTMS. Increases in the HDT and thermal stability and the presence of a slight nucleation effect with respect to PP crystallization were observed when 2 % fractions of clay were used, regardless of the compatibilizer type. The use of a compatibilizer promoted larger moduli in the PP nanocomposites but did not change the impact strength of the PP matrix, except for that observed in the 0.5 % OTMS and 1.5 % PP-*g*-MA system. The DMA results showed that the use of 1 wt% OTMS promoted the best adhesion between the OMMt and PP matrix system.

Acknowledgements The authors are grateful to CAPES, CNPq, Finep, and FAPERGS/PRONEX for their financial support.

References

1. Pavlidou S, Papaspyrides CD (2008) Prog Polym Sci 33:1119
2. Paul DR, Robeson LM (2008) Polymer 49:3187
3. Santos KS, Bischoff E, Liberman SA, Oviedo MAS, Mauler RS (2011) Ultrason Sonochem 18(5):997
4. Santos KS, dal Castel C, Liberman SA, Oviedo MAS, Mauler RS (2011) J Appl Polym Sci 119(3):1567
5. Chinellato AC, Vidotti SE, Hub G-H, Pessan LA (2010) Compos Sci Technol 70:458
6. Kandola BK, Smart G, Horrocks AR, Joseph P, Zhang S, Hull TR, Ebdon J, Hunt B, Cook A (2008) J Appl Polym Sci 108:816
7. Zeng QH, Yu AB, Lu GQ, Paul DR (2005) J Nanosci Nanotech 5:1574
8. Furlan LG, Ferreira CI, dal Castel C, Santos KS, Mello ACE, Liberman AS, Oviedo MAS, Mauler RS (2011) Mater Sci Eng, A 528(22–23):6715
9. Santos KS, Liberman SA, Oviedo MAS, Mauler RS (2008) J Polym Sci, Part B 46(23):2519
10. Santos KS, Liberman SA, Oviedo MAS, Mauler RS (2009) Compos A 40:1199
11. Dong Y, Bhattacharyya D (2008) Compos A 39:1177
12. Wang K, Wang L, Wu J, Chen L, He C (2005) Langmuir 21:3613
13. Lertwimolnun W, Vergnes B (2005) Polymer 46:3462
14. Ou B, Li D, Liu Y (2009) Compos Sci Technol 69:421
15. Garcia-Lopez D, Picazo O, Merino JC, Pastor JM (2003) Europ Polym J 39:945
16. Ding C, He H, Guo B, Jia D (2008) Polym Compos 29:698
17. Dong Y, Bhattacharyya D (2010) Mater Sci Eng, A 527:1617
18. Xu W, Liang G, Wang W, Tang S, He P, Pan W-P (2003) J Appl Polym Sci 88:3225
19. Wang Y, Chen F-B, Wu K-C (2005) J Appl Polym Sci 97:1667
20. Palza H, Vergara R, Yazdani-Pedram M, Quijada R (2009) J Appl Polym Sci 112:1278
21. Felix AHO, Cardozo NSM, Nachtigall SMB, Mauler RS (2006) Macromol Mater Eng 291:418
22. Li J, Ton-That M-T, Tsai S-J (2006) Polym Eng Sci 46:1060
23. Moncada E, Quijada R, Lieberwirth I, Yazdani-Pedram M (2006) Macromol Chem Phys 207:1376
24. Sanchez-Valdes S, Mendez-Nonell J, Medellin-Rodriguez FJ, Ramirez-Vargas E, Martinez-Colunga JG, Soto-Valdez H, Munoz-Jimenez L, Neira-Velazquez G (2009) Polym Bull 63:921
25. Spencer MW, Hunter DL, Knesek BW, Paul DR (2011) Polymer 52:5369
26. Salehi-Mobarakeh H, Yadegari A, Khakzad-Esfahlan F, Mahdavian A (2012) J Appl Polym Sci 124(2):1501
27. Chow WS, Neoh SS (2009) J Appl Polym Sci 114:3967
28. Herrera NN, Letoffe J-M, Putaux J-L, David L, Bourgeat-Lami E (2004) Langmuir 20(5):1564
29. Kim J-T, Lee D-Y, Oh T-S, Lee D-H (2003) J Appl Polym Sci 89:2633
30. Piscitelli F, Posocco P, Toth R, Fermeglia M, Pricl S, Mensitieri G, Lavorgna M (2010) J Coll Interf Sci 351:108
31. Mansoori Y, Atghia SV, Zamanloo MR, Imanzadeh G, Sirousazar M (2010) Europ Polym J 46:1844
32. Subramani S, Lee J-Y, Choi S-W, Kim JH (2007) J Polym Sci, Part B 45:2747
33. dal Castel C, Pelegrini T Jr, Barbosa RV, Liberman SA, Mauler RS (2010) Compos A 41:185
34. Nachtigall SMB, Miotto M, Schneider EE, Mauler RS, Forte MMC (2006) Eur Polym J 42(5):990
35. Park S-J, Kim B-J, Seo D-I, Rhee K-Y, Lyu Y-Y (2009) Mater Sci Eng, A 526:74
36. Shim JH, Joo JH, Jung SH, Yoon J-S (2007) J Polym Sci, Part B 45:607
37. Lu H, Hu Y, Li M, Chen Z, Fan W (2006) Compos Sci Technol 66:3035
38. Liaw W-C, Huang P-C, Chen C-S, Lo C-L, Chang J-L (2008) J Appl Polym Sci 109:1871
39. Amash A, Zugenmaier P (1997) J Appl Polym Sci 63:1143

40. Scobbo JJ (2000) In: Paul DR, Bucknall CB (eds) Polymer blends, vol 2. Wiley, New York, p 335
41. Martins CG, Larocca NM, Paul DR, Pessan LA (2009) Polymer 50:1743
42. Kim DH (2007) Polymer 48:5308
43. Chavarria F, Paul DR (2004) Polymer 45:8501
44. Yu Z–Z, Dasari A, Mai Y-W (2007) In: Advani SG (ed) Processing and properties of nanocomposites. World Scientific Publishing Co. Pte. Ltd, Singapore, p 310